Detecting Recurrent or Residual Lung Cancer with FDG-PET

Tomio Inoue, E. Edmund Kim, Ritsuko Komaki, Franklin C.L. Wong, Pedro Bassa, Wai-Hoi Wong, David J. Yang, Keigo Endo and Donald A. Podoloff

Departments of Nuclear Medicine and Radiotherapy, The University of Texas M.D. Anderson Cancer Center, Houston, Texas; Department of Nuclear Medicine, Gunma University School of Medicine, Maebashi, Japan; and Department of Nuclear Medicine, Hospital Clinic de Barcelona, University School of Medicine, Barcelona, Spain

We investigated the diagnostic accuracy of FDG-PET in the detection of recurrent lung cancer. **Methods:** Thirty-nine lesions in 38 patients with clinically suspected recurrent or residual lung cancer were studied with PET. All PET images were visually interpreted in conjunction with thoracic CT or MRI. Semiquantitative analysis using standardized uptake values (SUVs) was also performed in 25 lesions. FDG-PET diagnoses were correlated with pathological diagnoses and clinical outcome. **Results:** The sensitivity and specificity of FDG-PET for detecting recurrent tumors were 100% (26/26) and 61.5% (8/13), respectively. The difference in mean SUV between recurrent tumors and noncancerous lesions was statistically significant [11.2 ± 5.7 (n = 16) vs. 3.5 ± 1.8 (n = 9), $p < 0.0001$]. False-positive results showed relatively lower SUVs than true-positives and also demonstrated increased uptake in a curvilinear rather than nodular shape. **Conclusion:** FDG-PET is useful for detecting recurrent lung cancer after treatment. False-positive diagnoses might be reduced by analysis of uptake shape and serial changes in SUV, but further study is needed.

Key Words: positron emission tomography; fluorodeoxyglucose; lung cancer; recurrent lung cancer

J Nucl Med 1995; 36:788–793

PET with 2-[^{18}F]fluoro-2-deoxy-D-glucose (FDG) has been useful for the initial diagnosis (*1–6*) and staging (*7*) of lung cancer, although most lung cancer lesions can be detected by conventional chest radiography and thoracic CT or MRI. Noninvasive conventional imaging modalities may provide excellent morphological information for the detection of primary or metastatic lesions, but these modalities often cannot provide helpful information in differentiating recurrent or residual tumors from post-treatment changes (*8–10*).

We evaluated PET with FDG in the detection of recurrent disease in patients who had undergone various treatments for primary lung cancer.

Received Oct. 3, 1994; revision accepted Jan. 31, 1995.

For correspondence or reprints contact: E. Edmund Kim, MD, Department of Nuclear Medicine, The University of Texas M.D. Anderson Cancer Center, 1515 Holcombe Blvd., Houston, TX 77030.

MATERIALS AND METHODS

Patients

Thirty-eight patients (29 men and 9 women; age range, 37 to 80 yr) treated for primary lung cancer were included in this study. Pathological diagnoses of the primary tumor were established in all patients: 15 had adenocarcinoma, 14 squamous-cell carcinoma, 3 small-cell cancer, 3 large-cell cancer, 1 alveolar cell cancer, 1 nonsmall cell cancer and 1 carcinoma of unknown cell type. Local treatments were as follows: 12 patients had surgery and radiation therapy, 22 radiation therapy and 3 surgery. Twenty-two patients received systemic chemotherapy, including one patient treated with chemotherapy alone. Treatment was ended at least 3 mo prior to entry into this study.

Since one patient (Patient 13) had a lesion in each lung, 39 lesions were evaluated in this study. Thirty-six lesions were in the lung parenchyma and three lesions (Patients 1, 4, 13) were in the hilar area. Twenty-six lesions were recurrent or residual lung cancer; six of these lesions were diagnosed based on pathological findings, and 20 were diagnosed based on clinical symptoms, and signs (e.g., tumor marker levels) and radiographic evidence of disease progression on chest radiographs or CT or MRI. Thirteen lesions were noncancerous, five were diagnosed based on pathological findings and eight were diagnosed based on results of follow-up clinical and radiological examinations performed more than 6 mo after the PET scan.

There was one patient (Patient 34) with diabetes mellitus whose blood glucose level was well controlled during the PET study.

PET

FDG was produced in the cyclotron facility at The University of Texas M.D. Anderson Cancer Center by proton irradiation of enriched ^{18}O-water in a small-volume titanium target. Under sterile conditions, 2-deoxy-D-glucose was labeled with ^{18}F to produce FDG by the Hamacher method (*11*) using an automated system developed at our institute.

PET was performed with a Posicam 6.5 (Positron Corporation, Houston, TX) that provides a 42-cm field of view (FOV), 11 cm axial FOV and simultaneously acquires 21 slices with 5.1 mm slice thickness. The reconstructed transaxial and axial resolutions are 5.8 and 11.9 mm FWHM, respectively. Sensitivity is approximately 120,000 cps/μCi/ml. Image data were acquired with wobbling detectors and transferred to an independent Posicam data acquisition system.

Transmission scans were obtained with 185 MBq (5 mCi) of ^{68}Ga (approximately 300 million counts in 30 min) for attenuation correction. Prior to the PET study, patients fasted for at least 4 hr,

at which time normal blood glucose levels were confirmed prior to the PET imaging by clinical laboratory tests. Blood glucose levels were not measured during PET study. After intravenous injection of 375 MBq (10 mCi) FDG, three consecutive sets of transaxial images of the chest, centered on the suspected lesion, were obtained. Each set of transaxial images included 21 slices and it took 20 min to obtain each set. Sagittal and/or coronal images were also reconstructed and standardized uptake values (SUVs) of the peak activity on the PET images obtained 40–60 min after FDG injection were calculated pixel-by-pixel. Image pixel size was 1.7 mm in a 256 × 256 array. Tumor SUVs could not be estimated in 13 patients because they underwent the PET study before the SUV calculating system had been established in our institute. The color-coded superimposed images of SUVs and transmission data were produced with the departmental network of IBM RS/6000 workstation under the UNIX operating system. The SUV, a semiquantitative index of tissue uptake of FDG, was computed as follows:

$$\text{SUV} = \text{PET activity}/(\text{injected dose}/\text{body weight}),$$

where PET activity is a calibrated dose measured in millicurie per milliliter (*12*).

Analysis

PET images were independently interpreted by two nuclear radiologists in conjunction with chest radiographs, CT or MRI and patient history. The images obtained 40–60 min after FDG injection were routinely displayed for analysis. PET images were visually inspected, and abnormally increased FDG uptake in the lesion compared with FDG uptake by surrounding normal tissue and by the corresponding area in the contralateral lung was interpreted as tumor recurrence. In four cases with discordant results of interpretation of PET images, final results were obtained by the consensus of two nuclear radiologists. The sensitivity, specificity, and accuracy of PET in detecting recurrent lung cancer were determined by correlating PET diagnoses with pathological results in 13 lesions and with clinical outcomes in all patients.

The SUVs of the peak activity in the lesion were obtained from the SUV color-coded images. SUVs of less than 2.0 were estimated as 2.0 for convenient statistical analysis. The difference in mean SUVs between the recurrent tumors and noncancerous lesions was evaluated for statistical significance using the Mann-Whitney U-test. A p value of less than 0.01 was considered significant. The relationship of the threshold SUV in the lesion and the diagnostic accuracy in differentiating recurrent or residual tumor from post-treatment changes was also assessed in 25 lesions retrospectively.

RESULTS

Patient characteristics, lesion appearance on CT and MRI, lesion size measured on CT or MRI, PET findings and clinical/pathological findings are shown in Table 1. The size of suspicious lesions ranged from 2 × 2 × 2 cm to 9 × 6 × 8 cm on CT or MRI images. There were five false-positive PET diagnoses: two lesions (Patients 6, 17) that were proven to be acute inflammation on pathological examination; one lesion (Patient 35) for which fine-needle aspiration performed 2 yr after the PET study showed no malignant tumor cells; one instance (Patient 13) of false-positive uptake of FDG in the right lung base posteriorly without a mass lesion (with true-positive uptake in the left hilar lesion) (Fig. 1); and one lesion (Patient 5) for which fine-needle aspiration performed 1 and 8 mo after the PET study showed reactive mesothelial cells. False-positive FDG uptake in Patients 6 and 13 were in a curvilinear rather than focal nodular configuration (Fig. 2). All six lesions proved to be recurrent tumors by pathological or cytological diagnosis were detected by PET. Two lesions of hilar area (Patient 1, 13) were true-positive and the other one (Patient 4) was true-negative.

Sensitivity, specificity and accuracy of FDG-PET based on visual inspection were 100% (26/26), 61.5% (8/13), and 87.2% (34/39), respectively (Table 2).

The maximum SUV in the recurrent tumors ranged from 3.0 to 25.8 with a mean ± s.d. of 11.2 ± 5.7 (n = 16) and in the noncancerous lesion ranged from 2.0 to 7.5 with a mean ± s.d. of 3.5 ± 1.8 (n = 9) (Fig. 3). The SUV was significantly higher in the recurrent tumors ($p < 0.0001$; Mann-Whitney U-test). The SUV in cancerous lesions in patients with adenocarcinoma ranged from 7.5 to 25.8 with a mean ± s.d. of 11.4 ± 6.8 (n = 7), in patients with squamous-cell carcinoma ranged from 6.0 to 14.0 with a mean ± s.d. of 10.0 ± 3.3 (n = 4) and in patients with small-cell cancer ranged from 3.0 to 14.0 with a mean ± s.d. of 10.3 ± 6.4 (n = 3). There were no significant differences among three histologic types.

The relationship of the threshold SUV and diagnostic accuracy in differentiating recurrent or residual tumor from post-treatment changes is shown in Table 3. In contrast to the result from visual interpretations in the same subjects (sensitivity 100%, specificity 55.6%, accuracy 84%), a threshold SUV of 5.0 (a lesion with an SUV of less than 5.0 was considered noncancerous) provided optimal diagnostic accuracy (sensitivity 93.8%, specificity 88.9%, accuracy 92.0%).

DISCUSSION

In our study, there were 27 of 39 lesions for which the confirmation of noncancerous versus cancerous lesions occurred during clinical follow-up. This is a limitation of this study, but clinical follow-up is a valid way to evaluate response to therapy with this technique because 20 lesions diagnosed as cancerous showed a 30% increase in diameter on chest radiographs or CT as well as negative response to therapy after the PET study. Also, eight noncancerous lesions shown on chest x-rays, CT and MRI were stable more than 6 mo after PET study.

Since many rapidly growing tumor cells exhibit increased glycolysis (*13*), FDG has been proposed as an agent for tumor detection (*14*). FDG uptake in tumor cells is increased by elevated levels of glucose transporter messenger RNA induced by some oncogenes (*15*). Concentrations of hexokinase in tumor cells are also significantly correlated with measured growth rates and parallel the degree of loss of histological differentiation of tumor cells (*16*). These metabolic changes in tumor cells may be the principal mechanisms that make FDG-PET useful in the

TABLE 1
Patient Characteristics, Lesion Appearance on CT/MRI, Lesion Size, PET Findings and Clinicopathological Findings

Patient no.	Age	Sex	Original histology	Method of local treatment	Time since initial diag. (mo)	Lesion appearance on CT/MRI	Lesion size (cm)	SUV	PET diagnosis	Method of final diagnosis	Result
Nonsmall-cell Lung Cancer											
1	52	M	Adeno	RT	6	ILL-INF	3 × 7 × 13	7.5	Recurrence	CL	TP
2	55	M	Adeno	OP + RT	72	WELL-NOD	2 × 2.5 × 2		Recurrence	BB	TP
3	80	F	Adeno	OP	165	SP-NOD	3 × 3 × 3		Recurrence	OP	TP
4	58	F	Adeno	RT	14	SP-NOD	3 × 3 × 3.5		Negative	CL	TN
5	43	F	Adeno	OP + RT	18	ILL-INF	5 × 4 × 4	3.0	Recurrence	FNA	FP
6	50	F	Adeno	OP + RT	32	ILL-INF	4 × 5 × 5	5.0	Recurrence	BB	FP
7	63	M	Adeno	RT	28	ILL-INF	6 × 6 × 7.5	25.8	Recurrence	CL	TP
8	63	M	Adeno	RT	8	DONUT	3 × 4 × 5	14.0	Recurrence	CL	TP
9	44	M	Adeno	RT	5	ILL-INF	3 × 4 × 2	3.5	Negative	CL	TN
10	53	M	Adeno	OP + RT	55	SP-NOD	4 × 4 × 2		Recurrence	CL	TP
11	66	M	Adeno	RT	29	ILL-INF	3 × 4 × 4	7.5	Recurrence	CL	TP
12	39	M	Adeno	RT	10	SP-NOD	4 × 4 × 5	10.0	Recurrence	PLE	TP
13*	62	M	Adeno	OP + RT	31	SP-NOD	3 × 2 × 4		Recurrence	BF	TP
						ILL-INF	5 × 2 × 4		Recurrence	PLE	FP
14	54	M	Adeno	RT	24	ILL-INF	8 × 7 × 5	7.8	Recurrence	CL	TP
15	51	M	Adeno	RT	6	SP-NOD	3 × 3 × 4	7.5	Recurrence	CL	TP
16	65	M	SCC	OP + RT	41	ILL-INF	9 × 6 × 8	10.0	Recurrence	CL	TP
17	62	M	SCC	RT	12	CAVIT	8 × 6 × 6	7.5	Recurrence	BW	FP
18	74	F	SCC	OP + RT	11	DONUT	5 × 5 × 10		Recurrence	FNA	TP
19	55	F	SCC	RT	22	SP-NOD	2 × 3 × 3	2.0	Negative	CL	TN
20	65	F	SCC	OP + RT	26	DONUT	4 × 5 × 8	14.0	Recurrence	CL	TP
21	69	M	SCC	RT	10	ILL-INF	4 × 4.5 × 5	10.0	Recurrence	CL	TP
22	73	M	SCC	OP	15	SP-NOD	2.5 × 2.5 × 2		Negative	CL	TN
23	80	M	SCC	RT	24	CAVIT	6 × 7 × 6		Recurrence	BB	TP
24	64	M	SCC	RT	13	ILL-INF	4 × 5 × 12		Recurrence	CL	TP
25	54	M	SCC	OP	48	CONSO	8 × 8 × 5	2.0	Negative	CL	TN
26	80	M	SCC	RT	24	ILL-INF	6 × 7 × 5		Recurrence	CL	TP
27	74	M	SCC	RT	17	DONUT	6.5 × 6 × 7	6.0	Recurrence	CL	TP
28	68	M	SCC	OP + RT	21	ILL-INF	4.5 × 5 × 4		Recurrence	CL	TP
29	46	M	SCC	OP + RT	33	ILL-INF	3 × 4.5 × 4		Negative	CL	TN
30	59	M	Large cell	RT	9	ILL-INF	4 × 3 × 4	3.5	Negative	CL	TN
31	75	M	Large cell	RT	13	SP-NOD	2 × 2 × 2	20.0	Recurrence	CL	TP
32	68	M	Large cell	RT	6	SP-NOD	3 × 3 × 4		Recurrence	CL	TP
33	63	M	Non-small	RT	6	ILL-INF	4 × 4 × 4	7.5	Recurrence	CL	TP
34	71	F	ALV	OP + RT	65	SP-NOD	3 × 3 × 3	2.0	Negative	CL	TN
35	56	F	Unknown	OP + RT	42	ILL-INF	4 × 4 × 3	3.0	Recurrence	FNA	FP
Small-cell Lung Cancer											
36	70	M	Small cell	RT	14	ILL-INF	5 × 5 × 10	3.0	Recurrence	BW	TP
37	37	M	Small cell	RT	12	ILL-INF	5 × 7 × 7	14.0	Recurrence	CL	TP
38	69	M	Small cell		5	SP-NOD	5 × 6 × 5	14.0	Recurrence	CL	TP

*This patient had two separate lesions.

Adeno. = adenocarcinoma; ALV = alveolar cell cancer; RT = radiation therapy; OP = operation; ILL-INF = illdefined infiltration; WELL-NOD = well defined nodule; SUV = standardized uptake value; Unknown = unknown cell type; SCC = squamous cell carcinoma; SP-NOD = spiculated nodule or mass; DONUT = donut-shape lesion; CAVIT = cavitary lesion; CONSO = consolidation; CL = clinical course; FNA = fine needle aspiration; BB = bronchial brushing; BW = bronchial washing; PLE = cytology of pleural effusion; BF = findings of bronchofiber; TP = true-positive; TN = true-negative; FP = false-positive; FN = false-negative.

detection of malignant tumors. FDG uptake by the entire tumor is considered to be the result of uptake by both neoplastic and tumor-associated inflammatory components through active and passive mechanisms (*17,18*).

In our study, the SUV of FDG was significantly higher in recurrent tumors than in noncancerous lesions (Fig. 3). FDG-PET was also highly sensitive in detecting recurrent tumors. There were, however, five false-positive cases in which abnormally increased FDG uptake was misdiagnosed as recurrent cancer. Two patients showed acute inflammation (Patients 6, 17), and the others also showed components of reactive mesothelial cells (Patient 5) and pleural effusion (Patient 13). Similar results of accumulation of FDG in inflammatory lesions or newly formed granulation tissue have been reported (*2,19*).

Hilar and mediastinal lymph node are commonly involved by granulomatous disease and these lesions can have high FDG uptake. In this study, three lesions (Pa-

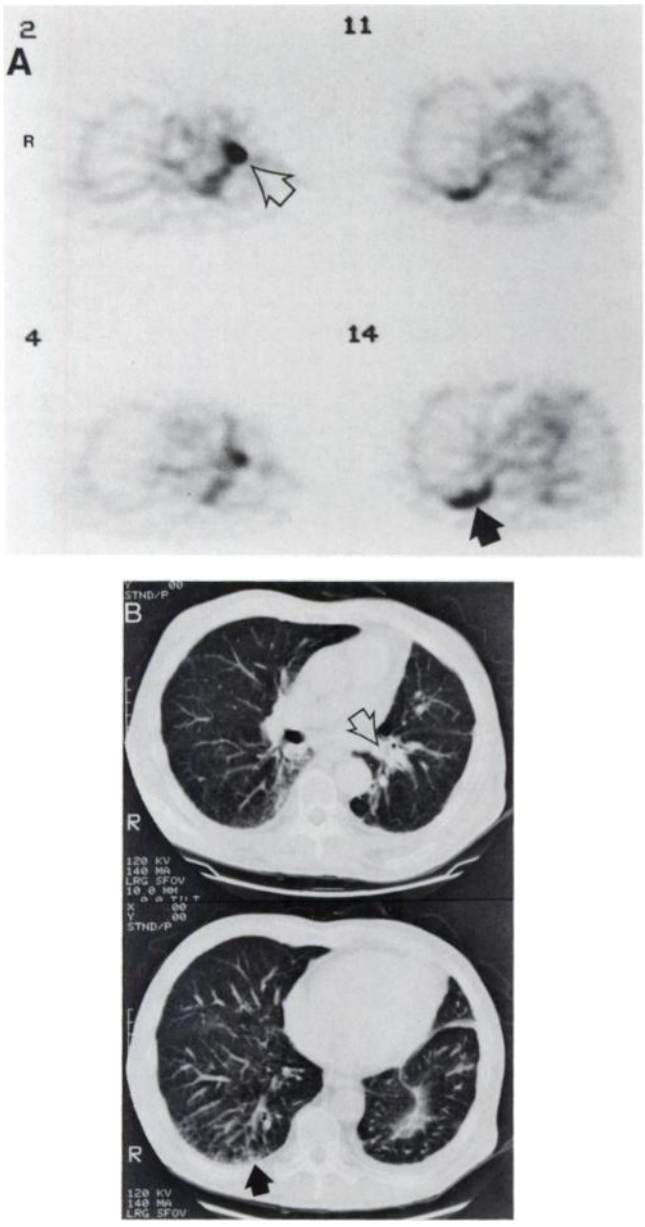

FIGURE 1. Patient 13, a 62-yr-old man with an adenocarcinoma. (A) FDG-PET image shows focal uptake (open arrow) in the hilar area of the left lung and curvilinear-shaped uptake (arrow) in the posterior base of the right lung. (The lower number indicates the higher slice level of the lung.) (B) CT demonstrates a possible nodule (open arrow) in the left hilar area and possible inflammatory changes (arrow) in the right posterior lung field. The right pleural effusion increased over the next few weeks, but the cultures and cytology were negative. Bronchoscopy of the left bronchus was suggestive of submucosal tumor invasion.

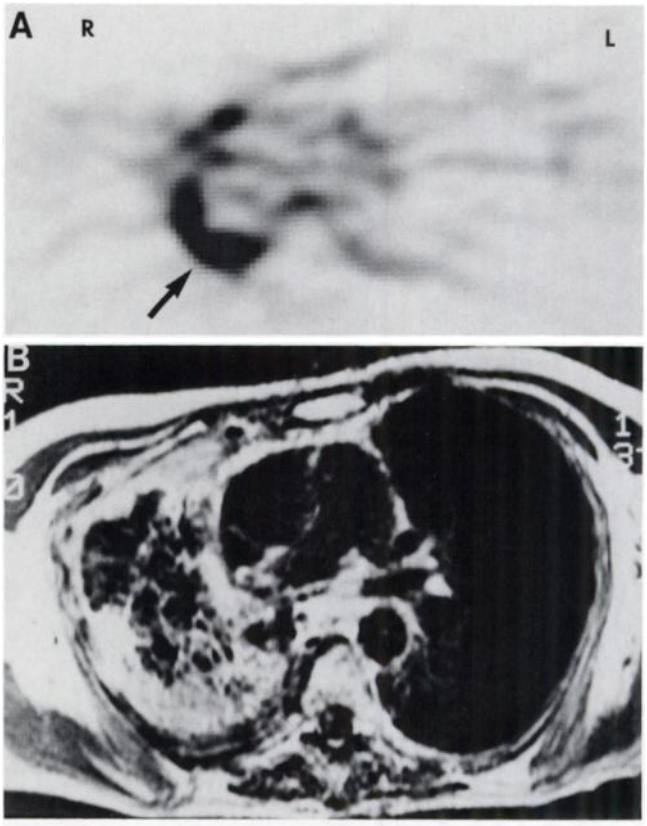

FIGURE 2. False-positive PET diagnosis in Patient 6, a 50-yr-old woman with adenocarcinoma. (A) Transaxial PET image of the chest shows markedly increased FDG uptake (arrow) along the right chest wall in a curvilinear shape. (B) MRI at the same level shows a mass around the right chest wall with bronchiectasis and atelectasis.

tients 1, 4, 13) were located in the hilar area, but none had false-positive results (Table 1). Radiation pneumonitis may also result in false-positive findings on FDG-PET since the pathological changes are associated with infiltration by macrophages, which have high FDG uptake (*17*). Radiation pneumonitis was not a cause of false-positive results in our study because the five patients with false-positive results underwent a PET study after more than 10 mo following the completion of radiotherapy.

Local tumor control is important to prevent metastatic dissemination and prolong survival (*20*). After the treatment of primary lung cancer, post-treatment changes sometimes interfere with the accurate radiological diagnosis of recurrent lung cancer (*9*). Some patients with suspected recurrent lung cancer undergo CT-guided needle biopsy, bronchoscopy, or thoracoscopic or open lung biopsy for pathological diagnosis, but these techniques are associated with complications and the possibility of sam-

TABLE 2
FDG-PET Differentiation of Recurrent Tumors from Post-Treatment Changes

PET diagnosis	Comprehensive diagnosis	
	Recurrence	No recurrence
Recurrence	26	5
No recurrence	0	8
Total	26	13

Sensitivity 26/26 = 100%; specificity 8/13 = 61.5%; accuracy 34/39 = 87.2%.

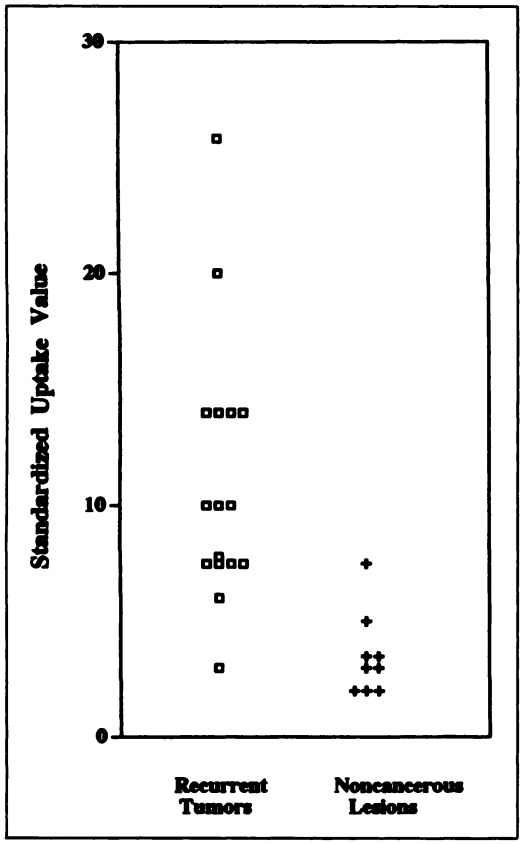

FIGURE 3. SUV distribution of FDG. SUV in recurrent tumors is significantly higher than that in noncancerous lesions.

pling errors (*21,22*). In this clinical setting, it would be extremely valuable if FDG-PET provided information on tumor viability (*23,24*). Our study suggests that FDG-PET may provide useful clinical information for selecting biopsy sites because of its high sensitivity in detecting recurrent lung cancer.

Patz et al. (*25*) reported that the sensitivity and specificity of FDG-PET for detecting recurrent lung tumors with a threshold SUV of 2.5 were 97.1% and 100%, respectively. In our study, FDG-PET also demonstrated a high sensitivity in detecting recurrent lung cancer, but we found a relatively lower specificity, even if a threshold SUV of 3.0 was used (Tables 2, 3). A threshold SUV of 5.0 seemed to provide the optimal diagnostic accuracy for detecting recurrent lung cancer in our patient population. This semiquantitative index, however, is affected by plasma glucose levels (*26*), tumor size, camera image resolution and image timing. For example, for a patient with small tumors, the SUV may be lower because of partial-volume averaging. Partial-volume averaging of SUVs in a lesion with a diameter less than 2 FWHM (1.2 × 1.2 × 2.4 cm in this study) should be considered, but only 2 of 25 lesions were subjects of the considerable effect of partial-volume averaging in our study in two patients. If the 5.0 SUV threshold is chosen, the lesion in Patient 36 becomes false-negative. Partial-volume averaging may not be a cause of false-negative results because of large lesion size. Other factors such as glucose level should be considered. Because plasma glucose levels may be affected during chemotherapy or glucocorticoid therapy in patients with lung cancer, a clinically practical method of quantitative analysis of FDG metabolic rates is needed (*27*).

TABLE 3
Results of Semiquantitative Analysis of PET Studies for Differentiation of Recurrent Tumors from Post-Treatment Changes

	% (No. of lesions)		
SUV Threshold	Sensitivity (%)	Specificity (%)	Accuracy (%)
<2.5	100 (16/16)	33.3 (3/9)	76.0 (19/25)
<3.0	93.8 (15/16)	55.6 (5/9)	80.0 (20/25)
<4.0	93.8 (15/16)	77.8 (7/9)	88.0 (22/25)
<5.0	93.8 (15/16)	88.9 (8/9)	92.0 (23/25)
<6.0	87.5 (14/16)	88.9 (8/9)	88.0 (22/25)
Visual analysis	100 (16/16)	55.6 (5/9)	84.0 (21/25)

SUV = standardized uptake values.

Nonsmall cell cancer and small-cell cancer are basically different diseases. In this study, SUVs of recurrent lesions in patients with small-cell cancer were not significant from those in patients with nonsmall cell carcinoma, such as squamous-cell carcinoma and adenocarcinoma. Further studies are needed to assess the differences in FDG-PET detection between recurrent nonsmall cell cancer and small-cell cancer because of the limited number of patients with small-cell cancer in our study.

In our experience, a curvilinear contour of increased FDG uptake was seen mostly in inflammatory lesions, while focal nodular uptake was seen mostly in recurrent tumors. The analysis of FDG distribution in the lesion may help us to differentiate recurrent cancer from post-treatment changes, but further study is needed.

In conclusion, FDG-PET is useful in the detection of recurrent lung cancer after treatment, but there are limitations in specificity. FDG-PET scans should be interpreted in conjunction with other anatomical images such as CT or MRI. Increased FDG uptake in suspicious lesions seen on CT, MRI or chest radiographs is most likely recurrent or residual lung cancer and additional therapy or confirmatory biopsy is required. Lesser or no FDG uptake indicates no recurrent lung cancer and follow-up with chest radiographs, CT or MRI is required. Semiquantitative and serial measurements of FDG uptake are needed in selected cases.

REFERENCES

1. Nolop KB, Rhodes CG, Brudin LH, et al. Glucose utilization in vivo by human pulmonary neoplasms. *Cancer* 1987;60:2682–2689.
2. Kubota K, Matsuzawa T, Fujiwara T, et al. Differential diagnosis of lung tumor with positron emission tomography: a prospective study. *J Nucl Med* 1990;31:1927–1933.
3. Gupta NC, Frank AR, Dewan NA, et al. Solitary pulmonary nodules: detection of malignancy with PET with 2-[F-18]-fluoro-2-deoxy-D-glucose. *Radiology* 1992;184:441–444.
4. Patz EF Jr, Lowe VJ, Hoffman JM, et al. Focal pulmonary abnormalities:

evaluation with ^{18}F fluorodeoxyglucose PET scanning. *Radiology* 1993;188: 487–490.
5. Strauss LG, Comti PS. The application of PET in clinical oncology. *J Nucl Med* 1991;32:623–648.
6. Rege SD, Hoh CK, Glaspy JA, et al. Imaging of pulmonary mass lesions with whole-body positron emission tomography and fluorodeoxyglucose. *Cancer* 1993;72:82–90.
7. Wahl RL, Quint LE, Greenough RL, Meyer CR, White RI, Orringer MB. Staging of mediastinal nonsmall cell lung cancer with FDG PET, CT and fusion images. Preliminary prospective evaluation. *Radiology* 1994;191: 371–377.
8. Glazer HS, Lee JKT, Levitt RG, et al. Radiation fibrosis: differentiation from recurrent tumor by MR imaging. *Radiology* 1985;156:721–726.
9. Glazer HS, Aronberg DJ, Sagel SS, Emami B. Utility of CT in detecting postpneumonectomy carcinoma recurrence. *Am J Roentgenol* 1984;142: 487–494.
10. Hatfield MK, MacMahon H, Ryan JW, et al. Postoperative recurrence of lung cancer: detection by whole-body gallium scintigraphy. *Am J Roentgenol* 1986;147:911–916.
11. Mamacher K, Coenen HH, Stocklin G. Efficient stereospecific synthesis of no-carrier-added [^{18}F]fluoro-2-deoxyglucose using aminopolyether supported nucleophilic substitution. *J Nucl Med* 1986;27:235–238.
12. Zasadny KR, Wahl RL. Standardized uptake values of normal tissues at PET with 2-[fluorine-18]-fluoro-2-deoxy-D-glucose: variations with body weight and a method for correction. *Radiology* 1993;189:847–850.
13. Warburg O. On the origin of cancer cells. *Science* 1956;123:309–314.
14. Som P, Atkins HL, Bandoypadhyay D, et al. A fluorinated glucose analog, 2-fluoro-2-deoxy-D-glucose(F-18): nontoxic tracer for rapid tumor detection. *J Nucl Med* 1980;21:670–675.
15. Flier JS, Mueckler MM, Usher P, Lodish HF. Elevated levels of glucose transport and transporter messenger RNA are induced by rats or src oncogenes. *Science* 1987;235:1492–1495.
16. Knox WE, Jamdar SC, Davis PA. Hexokinase, differentiation and growth rates of transplanted rat tumors. *Cancer Res* 1970;30:2240–2244.
17. Kubota R, Yamada S, Kubota K, et al. Intratumoral distribution of fluorine-18-fluorodeoxyglucose in vivo: high accumulation in macrophages and granulation tissues studied by microautoradiography. *J Nucl Med* 1992;33:1972–1980.
18. Kubota R, Kubota K, Yamada S, Tada M, Ido T, Tamahashi N. Active and passive mechanisms of [fluorine-18]fluorodeoxyglucose uptake by proliferating and prenecrotic cancer cells in vivo: a microautoradiographic study. *J Nucl Med* 1994;35:1067–1075.
19. Tahara T, Ichiya Y, Kuwabara Y, et al. High [^{18}F]-fluorodeoxyglucose uptake in abdominal abscesses: a PET study. *J Comput Assist Tomogr* 1989;13:829–831.
20. Suit HD. The scope of the problem of primary tumor control. *Cancer* 1988;61:2141–2147.
21. Haramati LB, Austin JHM. Complications after CT-guided needle biopsy through aerated versus nonaerated lung. *Radiology* 1991;181:778.
22. Austin JHM, Cohen MB. Value of having a cytopathologist present during percutaneous fine-needle aspiration biopsy of lung: report of 55 cancer patients and metaanalysis of the literature. *Am J Roentgenol* 1993;160:175–177.
23. Ichiya Y, Kuwabara Y, Otsuka M, et al. Assessment of response to cancer therapy using fluorine-18-fluorodeoxyglucose and positron emission tomography. *J Nucl Med* 1991;32:1655–1660.
24. Kim EE, Chung S-K, Haynie TP, et al. Differentiation of residual or recurrent tumors from posttreatment changes with F-18 FDG-PET. *Radiographics* 1992;12:269–279.
25. Patz EF Jr, Lowe VJ, Hoffman JM, Paine SS, Harris LK, Goodman PC. Persistent or recurrent bronchogenic carcinoma: detection with PET and 2-[F-18]-2-deoxy-D-glucose. *Radiology* 1994;191:379–382.
26. Langer KJ, Braun U, Kops ER, et al. The influence of plasma glucose levels on fluorine-18-fluorodeoxyglucose uptake in bronchial carcinomas. *J Nucl Med* 1993;34:355–359.
27. Wong W-H, Hicks K. A clinically practical method to acquire parametric images of unidirectional metabolic rates and blood spaces. *J Nucl Med* 1994;35:1206–1212.